JOURNAL OF MATERIALS SCIENCE 14 (1979) 1433–1439

The effect of heating on the domain structure of beta-eucryptite, $LiAlSiO_4$

W. F. MÜLLER
Fachbereich 11, Mineralogie, Technische Hochschule Darmstadt, D-6100 Darmstadt, Germany

Transmission electron microscopy of β-eucryptite revealed the occurrence of antiphase domains with the antiphase vector $\frac{1}{2}\mathbf{a}$. This vector relates (Si, Al)O_4-tetrahedra which are chemically equivalent, i.e. either SiO_4 or AlO_4 (in an ordered structure); therefore, it leaves the Si/Al long-range order undisturbed. The size of the domains depends on the temperature history of the crystals. Antiphase domains with the antiphase vector $\frac{1}{2}\mathbf{c}$ have not been observed. *In situ* heating experiments showed that the superstructure reflections of the type $h + k = 2n + 1$, $l = 2n + 1$ ("*a*-reflections") rapidly lose their intensity and become unobservable at temperatures around 550° C (furnace, not specimen temperature) as also known from X-ray studies of β-eucryptite at 460° C (specimen temperature). This change is reversible. Correspondingly, the antiphase domain boundaries which are imaged with the *a*-reflections disappear at these temperatures. Upon cooling, the antiphase domain boundaries reappear at the same positions as before. It is concluded that position, shape and size of the antiphase domains is controlled by the number and distribution of local defects in the Si/Al order.

1. Introduction

Beta-eucryptite, $LiAlSiO_4$, is an interesting material for at least two reasons: first, its structure is a stuffed derivative of high-quartz and displays order–disorder phenomena regarding its Si/Al distribution as well as its site occupancy of the Li-ions [1–16]. Second, its physical properties are unusual. The slightly negative thermal volume expansion [14, 17, 18] is the basis for the technical use of β-eucryptite as the main constituent (usually in solid solution) of glass ceramics with an extremely small thermal expansion [19]. The other rare physical property of β-eucryptite which was only recently discovered is the one-dimensional ionic conductivity [20–22].

The physical properties are closely related to the structure of β-eucryptite and are significantly influenced by the order–disorder of Li, Al and Si; the high mobility of the small Li-ions in structural channels is of special interest [14, 20]. Since physical and chemical properties are also influenced by the nature and microstructure of the crystal defects present in crystalline solids, a transmission electron microscope (TEM) study has been started. In a previous publication on defects in β-eucryptite, the occurrence of antiphase domains about 0.1 to 0.5 μm in size with the displacement vector $\frac{1}{2}\mathbf{a}$ has been discussed [23]. In the present paper we will report on the effect of heating on the domain structure as revealed by TEM.

2. Materials and techniques

Suitably thin specimens for TEM with 100 kV acceleration voltage were prepared from conventional petrographic thin sections of β-eucryptite by ion bombardment [24–26]. Specific conditions are described by Müller and Wenk [27]. TEM observations were made with a JEOL JEM 100 B electron microscope equipped with a side-entry goniometer. The commercial heating holder was used for heating experiments *in situ* since non-quenchable phenomena were suspected to occur. The TEM methods employed in this study for analysing crystal defects are described in textbooks in detail, e.g. Hirsch *et al.* [28], Amelinckx *et al.* [29], Wenk [30].

The crystals used in this study were grown from solution using a flux [1, 7, 22] and were kindly donated by Professor Heinz Schulz, Stuttgart. Four samples (a, b, c and d) have been investigated. The temperature history of samples a, b and d was not controlled. Sample c had been heated at 1140° C for 8 days.

3. Crystal structure

β-eucryptite is a stuffed derivative of the high-quartz structure [37], in which half the Si^{4+}-ions are replaced by Al^{3+}-ions. The charge is balanced by the incorporation of Li^{+}-ions into the (Si, Al)O_4 framework. Winkler [1] was the first to investigate the crystal structure. Symmetry and extinctions of the main reflections in single crystal X-ray photographs indicated the high-quartz space group $P6_222$ and weak superstructure reflections demanded a doubling of the high-quartz-like c-axis. Winkler correctly explained the doubling of the c-axis by an alternating sequence of Si and Al layers perpendicular to the c-axis. Buerger [2] also noted that the a-axes have to be doubled. More recently, the determination and discussion of the average and superstructure has been published in several papers [9–12, 15, 16]. The lattice constants of the hexagonal superstructure are $a = 10.5$ Å and $c = 11.2$ Å. On the basis of the supercell, the reflections can be classified as follows [12]:

(1) main reflections: $h = 2n$, $k = 2n$, $l = 2n$

(2) superstructure reflections:

(a) $h = 2n$, $k = 2n$, $l = 2n + 1$ (c-reflections)

(b) $h + k = 2n + 1$ or $h = 2n + 1$, $k = 2n + 1$, $l = 2n + 1$ (a-reflections)

(c) $h + k = 2n + 1$ or $h = 2n + 1$, $k = 2n + 1$ and $l = 2n$.

A characteristic feature of the structure are the channels parallel to the six-fold axis, which are formed by the (Si, Al)-O_4 framework and house the Li atoms. There are two sorts of crystallographic independent channels, namely one central channel and three symmetrically equivalent secondary channels which are separated from the central channel by $\frac{1}{2}\mathbf{a}_1$, $\frac{1}{2}\mathbf{a}_2$ or $\frac{1}{2}(\mathbf{a}_1 + \mathbf{a}_2)$, respectively (Fig. 1). The Si and Al atoms are ordered in alternating layers perpendicular to the c-axis. Each Al is surrounded by four Si and vice versa, in agreement with the Al avoidance principle [31, 32]. The Li atoms occupy, in an ordered way, sites co-ordinated by four oxygens. The Li atoms in the central channel have the same z co-ordinates as the Al atoms and the Li atoms in the three secondary channels have the same z co-ordinates as the Si atoms. The translation $\frac{1}{2}\mathbf{c}$ relates subcells with reversed Si, Al occupancy of tetrahedra. The translation $\frac{1}{2}\mathbf{a}$, however, relates Si- or Al-tetrahedra which are chemically equivalent.

X-ray studies have shown that the intensities of the a-reflections decrease with increasing temperature; at about 460° C the a-reflections become unobservable [7, 13]. When the crystal is cooled, these reflections appear again and, at room temperature, they reach about their original intensity. Main and c-reflections display only comparatively small changes in intensity due to the heating. The effect of heating on the a-reflections is attributed to a dynamic disordering process of the Li atoms [14]: the Li atoms can occupy sites which are surrounded by either four or six oxygens (Fig. 1). At room temperature the Li atoms are situated in the four-fold co-ordination polyhedra. With increasing temperature the Li atoms change sites.

At about 460° C all channels display the same statistical distribution of Li on the four- and six-fold co-ordinated lattice sites, e.g. the differences in the Li distribution between the central and secondary channels mentioned above (Fig. 1) decrease with increasing temperature and disappear at about 460° C.

The results of a recent study by means of

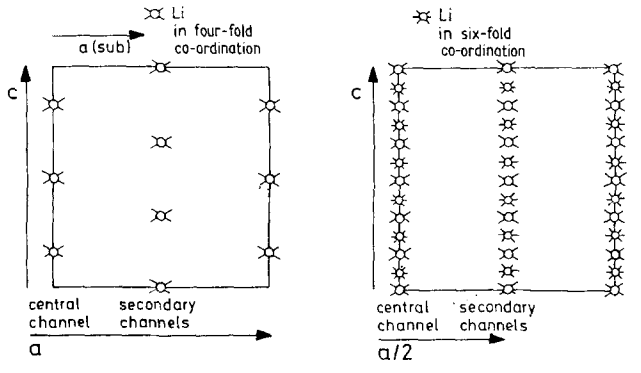

Figure 1 Ordered distribution of lithium atoms at room temperature (left) and their disordered distribution above 460° C (right) in β-eucryptite. After [4].

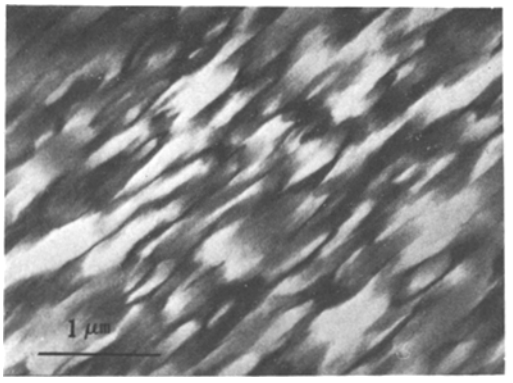

Figure 2 Antiphase domains with the antiphase vector $\frac{1}{2}\mathbf{a}$ in β-eucryptite. Note the preferred orientation of the domain boundaries parallel to c. Transmission electron micrograph of crystal a in dark-field mode using a reflection of the type $h + k = 2n + 1, l = 2n + 1$.

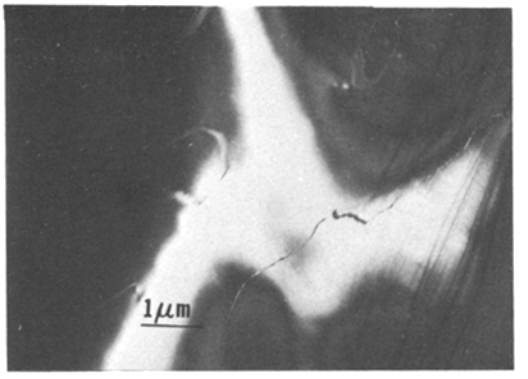

Figure 3 Large antiphase domains with the antiphase vector $\frac{1}{2}\mathbf{a}$ in β-eucryptite crystal c. Dark-field transmission electron micrograph.

neutron diffraction [16] confirm on the whole the structure model of the high temperature phase given in [10, 14] and are in agreement with X-ray structure determinations at room temperature [9–13].

4. TEM observations

4.1. Observations at room temperature

Samples a, b and c displayed antiphase domains. These were visible in dark-field mode with a-reflections operating and were found to be out of contrast when the main and type c-reflections were used. As already mentioned, the displacement vector of the antiphase domains is $\frac{1}{2}\mathbf{a}$ [23]. Samples a and b contain relatively small antiphase domains about 0.1 to 0.5 μm in size whose boundaries have a strong preferential orientation parallel to c (Fig. 2). The antiphase domains of sample c which had been heat-treated for 8 days are much larger and no preferred orientation is apparent (Fig. 3). Note in Fig. 3 that the antiphase domain boundaries (APBs) are not smooth but slightly ragged. The a-reflections of sample d were already diffuse at room temperature and no domains could be imaged.

The TEM work was severely hampered by the high sensitivity of β-eucryptite to electron irradiation. Even at a very moderate beam intensity, as is necessary for focusing the image and orienting the crystal for the proper imaging conditions, e.g. tilting the crystal so that a type a-reflection is strongly excited, type a-reflections and the superstructure reflections of the type $h + k = 2n + 1$ (or $h = 2n + 1$, $k = 2n + 1$) and $l = 2n$ became increasingly diffuse. The images shown in Figs. 2, and 3 were obtained by first adjusting the conditions at one area of the crystal and then moving to a neighbouring area which had not been irradiated before. With more intense electron irradiation the a-reflections disappear within seconds and after about a minute the c-reflections are no longer observable. These processes are not reversible. (It appeared that the β-eucryptite crystal with the large domains was much more resistant to electron irradiation.)

A sequence of diffraction patterns with increasing irradiation doses as described above is shown in Fig. 4. It can be seen from Fig. 4a that not only the a- and c-reflections are sharp and relatively intense but also the superstructure reflections of the type $h = 2n + 1, l = 2n$ can easily be observed. The latter are apparently not easy to record by standard X-ray methods [12].

According to the space group of β-eucryptite, reflections of the type $(0\,0\,0\,l)$ should only be present for $l = 3n$. In Fig. 4a this rule is apparently not obeyed. On the other hand, multiple diffraction is a common phenomenon in electron diffraction and especially systematic absences due to a screw axis are easily veiled by the occurrence of "forbidden" reflections due to this effect. However, in the present case, the reflections $l = 3n$ are much too strong to be solely due to double reflection and the space group of β-eucryptite at room temperature should be re-examined.

The diffraction pattern of Fig. 4b shows that the diffuse a-reflections are actually satellites, the diffuse diffraction maxima are streaked parallel to a^*. The superstructure reflections of the type $h = 2n + 1, l = 2n$ show the same effect but have now a much lower intensity than the a-reflections and are barely visible on the photographs.

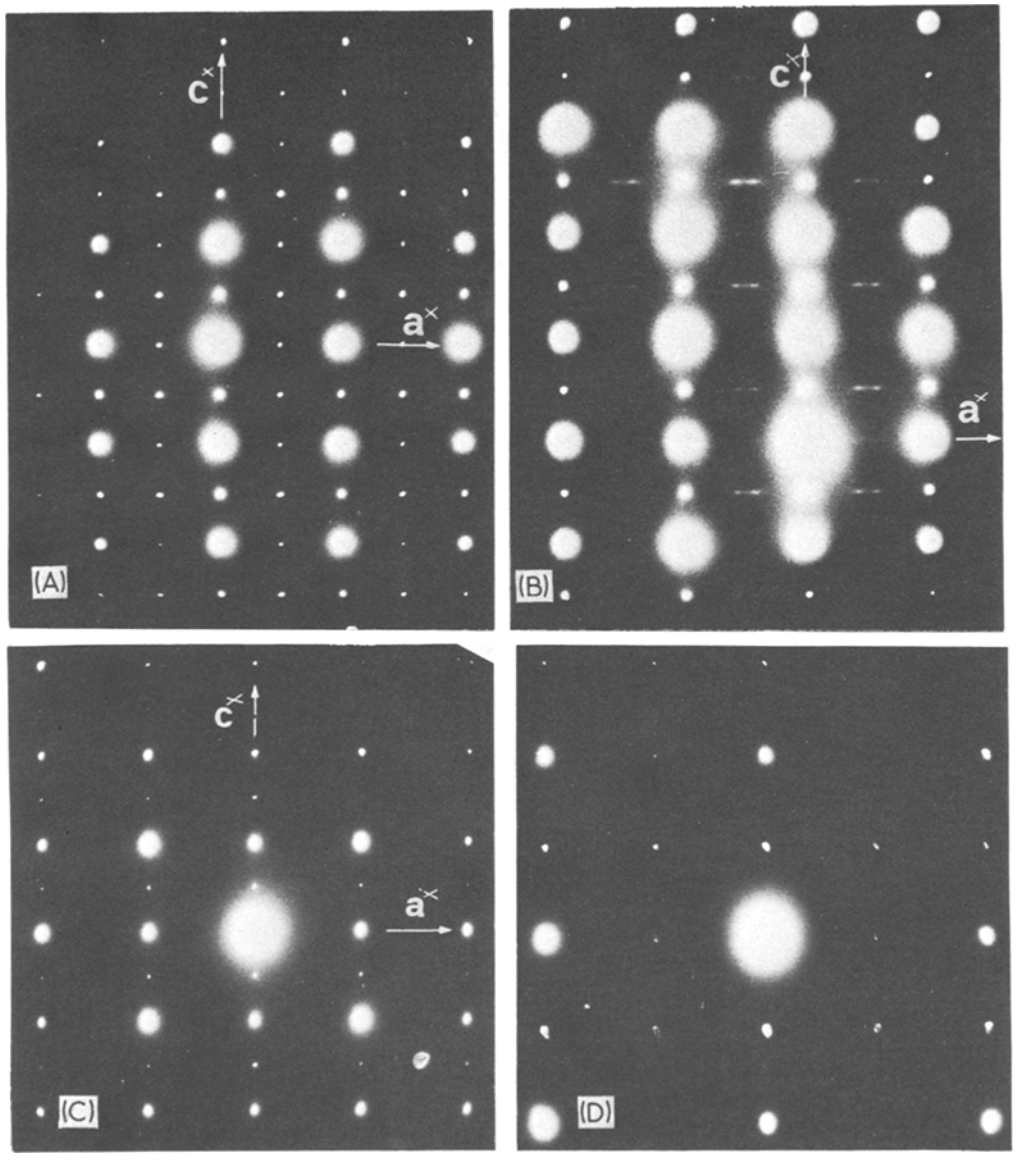

Figure 4 Effects of electron irradiation on the structure of β-eucryptite as revealed by electron diffraction patterns. The irradiation dose was as low as possible in (a) and was increased from (a) to (d).

4.2. *In situ* heating experiments

Heating experiments on β-eucryptite inside the electron microscope have been performed using the commercial heating holder. The temperatures given in the following refer to the temperature of the furnace; the actual temperature of the area under observation may be significantly lower (cf. [26]). Above about 550° C the reflections rapidly lose their sharpness and intensity and become unobservable on the viewing screen. However, on the original photographic plates it can be seen that the *a*-reflections are now replaced by a pair of very weak and diffuse satellites along a^*. Upon cooling, the *a*-reflections reappear and regain their sharpness and intensity at room temperature.

(Obviously, the sharp decrease of the intensity of the *a*-reflections around 550° C furnace temperature found in this electron diffraction study is due to the same phase change as observed in X-ray work around 440 to 460° C. Therefore, it is most probable that the intensity decrease reported here occurs at an actual specimen temperature of about 440 to 460° C). This is illustrated by Fig. 5 which shows electron diffraction patterns taken at various temperatures of crystal c. Fig. 5a displays the diffraction pattern at room temperature (20° C),

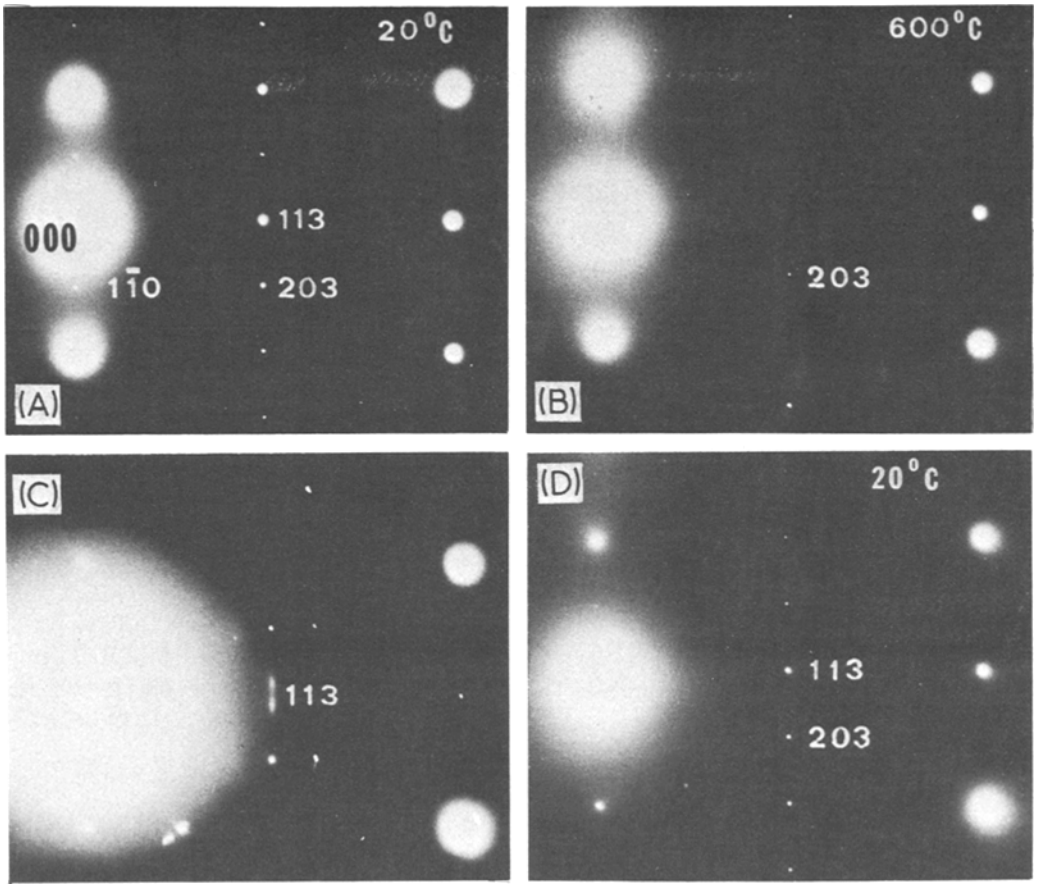

Figure 5 Electron diffraction patterns of β-eucryptite (crystal c) taken at various temperatures. (a) 20° C, (b) 600° C, (d) 20° C, after heating to 600° C and cooling to room temperature. (c) Intermediate temperature obtained during cooling from 600° C. See Section 4.2 for details.

Fig. 5d is a pattern taken at 20° C after heating to about 600° C and subsequent cooling. In the pattern of Fig. 5b recorded at 600° C, the *a*-reflection 1 1 3 has disappeared; the pair of very diffuse satellites is only visible on the original plate as mentioned above. The electron diffraction photograph of Fig. 5c displaying intense satellites at the position of 1 1 3 was taken at an intermediate temperature during cooling. It is likely that this type of satellite has been observed in X-ray photographs [15] and not those mentioned for Fig. 5b, since the latter are not restricted to a temperature interval of only 20° C [15].

Of special interest was the question of the effect of heating on the domains. As to be expected, the APBs became invisible at the moment the *a*-reflections lost their intensity and sharpness. However, when the crystal is cooled and the *a*-reflections are visible and sharp again, the APBs reappear. They reappear at the same positions they held before heating, i.e. they display a memory effect (Fig. 6).

5. Discussion

The fragmentation of crystals into antiphase domains mostly originates from sub-solidus phase transitions during cooling. The space group of the low-temperature phase (derived structure) is then a subgroup of the high temperature phase (parent structure) which has lost translational symmetry but possesses the same point group symmetry as the parent structure. The displacement vector, also called antiphase vector, of the antiphase domains has the direction and length of the translational symmetry operation lost as a consequence of the transition. (For more detailed discussions on the crystal chemical relevance of domains, see [33–37]).

In the case of β-eucryptite, the displacement vector of the antiphase domains observed is $\frac{1}{2}\mathbf{a}$. From this follows that the high temperature phase has an *a*-axis which is half that of the structure at room temperature.

The reader is reminded that the $\frac{1}{2}\mathbf{a}$ translation relates (Si, Al)O_4-tetrahedra which are chemically

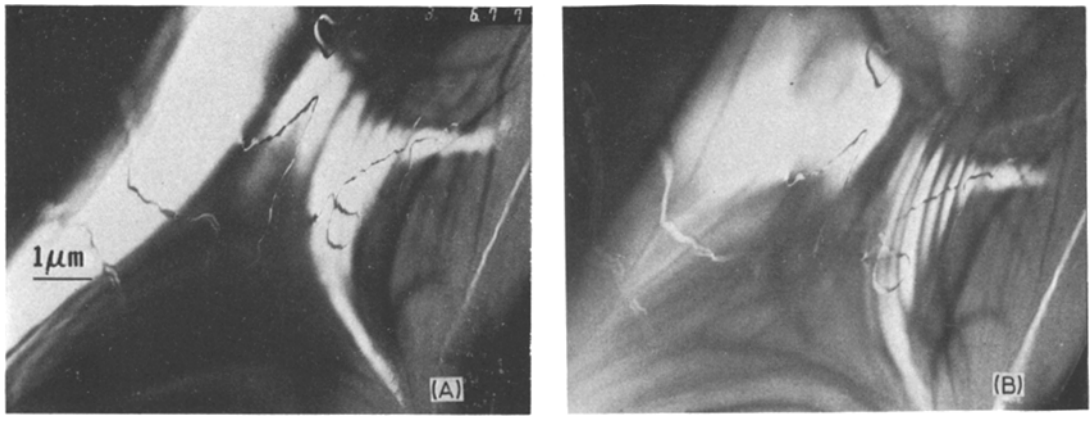

Figure 6 Antiphase domain boundaries with the antiphase vector $\frac{1}{2}\mathbf{a}$ in β-eucryptite before and after heating to 600° C. Note the memory effect of the antiphase domain boundaries.

equivalent, i.e. either SiO_4 or AlO_4. In other words, the translation $\frac{1}{2}\mathbf{a}$ leaves the Si/Al long-range order undisturbed; however, central and secondary channels are exchanged. Thus, the occurrence of antiphase domains is apparently closely connected with the phase transition at about 460° C. The observation of the memory effect of the antiphase domains reported in Section 4.2 indicates that the antiphase domain structure is controlled by a structural pattern occurs as local defects in the transition at about 460° C. It is suggested that this structureal pattern occurs as local defects in the Si/Al order (not in the long-range order), which are not removed by heating up to these relatively low temperatures. This interpretation also explains the different domain sizes in the various samples: suitable heat-treatment at very high temperatures just below the crystal temperature at which ordering of Si/Al begins and slow cooling will yield a highly ordered Si/Al-distribution; the antiphase domains will become large. Rapid cooling through the critical temperature at which Si/Al ordering begins will produce a high degree of local Si/Al disorder: small domains are the result.

The other type of antiphase domains with the displacement vector $\frac{1}{2}\mathbf{c}$ which can be imagined to occur in β-eucryptite has not been observed in our samples. These antiphase domains should form in crystals with an originally statistical distribution of Al and Si.

Some of the properties and behaviour of β-eucryptite resemble those known for the Ca-feldspar, $CaAl_2Si_2O_8$. Anorthite which is also a framework aluminium silicate with an Si : Al ratio of 1 : 1 displays order–disorder phenomena due to the ordering of Si and Al in agreement with the Al-avoidance principle and rattling of Ca in the large interstices of the framework. When heated above 150° C, the superstructure reflections of the type $h + k + l = 2n + 1$ become increasingly diffuse as shown by X-ray methods; diffuse reflections of this type have been observed by X-rays even at temperatures as high as 1500° C. (Extensive information on anorthite is given by Smith [38]; see also Jagodzinski and Korekawa [39].) However, elastic neutron diffraction data proved that anorthite undergoes a reversible phase transition at 237° C from a primitive to a body-centred structure [40]. TEM methods have shown that anorthite contains APBs with the displacement vector $\frac{1}{2}(\mathbf{a} + \mathbf{b} + \mathbf{c})$ which can be imaged with reflections of the type $h + k + l = 2n + 1$. The size of domains depends on the cooling history. When heated to a few hundred degrees these APBs disappear but reappear after cooling without any change in position and shape [27] analogous to the behaviour of the APBs in β-eucryptite. It is probable that, as in the case of anorthite, distribution and frequency of local substitutional Si/Al disorder is responsible for the domain structure [27, 41]. Those antiphase domains originating from the long-range ordering of Si/Al at high temperatures, which have not been observed in β-eucryptite so far, commonly occur in natural and synthetic anorthite crystallized from the melt (cf. [42]) or from glass [43].

Finally, some of the problems touched upon but not solved by this study are briefly mentioned: these are, in particular, the origin and nature of the satellites, the character of the transition at 460° C, and the question of the space group of β-eucryptite at room temperature. Of special inter-

est would be whether the conductivity properties of β-eucryptite are correlated with the domain microstructure and, if so, by what means.

Acknowledgements

The author thanks Professor Heinz Schulz for helpful discussions and donation of crystals and Professor Masaaki Korekawa for his interest in this work. Support by the Deutsche Forschungsgemeinschaft is gratefully acknowledged. The experimental work was carried out at the Institut für Kristallographie und Mineralogie of the Goethe-Universität, Frankfurt am Main.

References

1. H. G. F. WINKLER, *Acta Cryst.* **1** (1948) 27.
2. M. J. BUERGER, *Amer. Mineral.* **33** (1948) 751.
3. *Idem, ibid* **39** (1954) 600.
4. M. BEHRUZI and Th. HAHN, *Naturwiss.* **54** (1967) 643.
5. *Idem, Z. Kristallogr.* **133** (1971) 405.
6. *Idem, Fortschr. Mineral.* **55** Beiheft 1 (1977) 12.
7. V. TSCHERRY and F. LAVES, *Naturwiss.* **57** (1970) 194.
8. V. TSCHERRY and H. SCHULZ, *ibid* **57** (1970) 194.
9. H. SCHULZ and V. TSCHERRY, *Acta Cryst. B* **28** (1972) 2168.
10. *Idem, ibid* **28** (1972) 2174.
11. V. TSCHERRY, H. SCHULZ and F. LAVES, *Z. Kristallogr.* **135** (1972) 161.
12. *Idem, ibid* **135** (1972) 175.
13. W. W. PILLARS and D. R. PEACOR, *Amer. Mineral.* **58** (1973) 681.
14. H. SCHULZ, *J. Amer. Ceram. Soc.* **57** (1974) 313.
15. U. v. ALPEN, H. SCHULZ, G. H. TALAT and K. H. THIEMANN, *Z. Kristallogr.* **146** (1977) 89.
16. H. GUTH and G. HEGER, *ibid* **146** (1977) 143.
17. F. A. HUMMEL, *J. Amer. Ceram Soc.* **34** (1951) 235.
18. F. H. GILLERY and E. A. BUSH, *ibid* **42** (1959) 175.
19. J. PETZOLDT, *Glastech. Ber.* **40** (1967) 385.
20. H. BÖHM, *Phys. Stat. Sol. (a)* **30** (1975) 531.
21. R. T. JOHNSON JUN., B. BOROSIN, M. L. KNOTEK and R. M. BIEFELD, *Phys. Letters* **54A** (1975) 403.
22. U. v. ALPEN, E. SCHÖNHERR, H. SCHULZ and G. H. TALAT, *Electrochim. Acta* **22** (1977) 805.
23. W. F. MÜLLER and H. SCHULZ, *Naturwiss.* **63** (1976) 294.
24. H. BACH, *Bosch Techn. Berichte* **1** (1964) 10.
25. D. J. BARBER, *J. Mater. Sci.* **5** (1970) 1.
26. N. J. TIGHE, "Electron Microscopy in Mineralogy", edited by H. R. Wenk (Springer-Verlag, Berlin, Heidelberg, New York, 1976) p. 144.
27. W. F. MÜLLER and H. -R. WENK, *N. Jb. Miner. Mh.* (1973) 17.
28. P. B. HIRSCH, A. HOWIE, R. B. NICHOLSON, D. W. PASHLEY and M. J. WHELAN, "Electron Microscopy of Thin Crystals" (Butterworths, London, 1965).
29. S. AMELINCKX, R. GEVERS, G. REMAUT and J. VAN LANDUYT (Eds.) "Modern Diffraction and Imaging Techniques in Materials Science" (North Holland Press, Amsterdam, 1970).
30. H. R. WENK (coordinating Ed.), "Electron Microscopy in Mineralogy" (Springer-Verlag, Berlin, Heidelberg, New York, 1976).
31. W. LOEWENSTEIN, *Amer. Mineral.* **39** (1954) 92.
32. J. R. GOLDSMITH and F. LAVES, *Z. Kristallogr.* **106** (1955) 213.
33. S. AMELINCKX and J. VAN LANDUYT, "Electron Microscopy in Mineralogy" edited by H. -R. Wenk (Springer-Verlag, Berlin, Heidelberg, New York, 1976) p. 68.
34. H. BÄRNIGHAUSEN, *Acta Cryst. A* **31** Suppl. (1975) p. S 3.
35. *Idem*, private communication (1975).
36. G. VAN TENDELOO and S. AMELINCKX, *Acta Cryst. A* **31** (1975) 431.
37. J. WONDRATSCHEK and W. JEITSCHKO, *ibid* **A32** (1976) 664.
38. J. V. SMITH, "Feldspar Minerals", Vol. 1 (Springer-Verlag, Berlin, Heidelberg, New York, 1974).
39. H. JAGODZINSKI and M. KOREKAWA, *Z. Kristallogr.* **143** (1976) 239.
40. F. FREY, H. JAGODZINSKI, W. PRANDL and W. B. YELON, *Phys. Chem. Minerals* **1** (1977) 227.
41. F. LAVES and J. R. GOLDSMITH, *Acta Cryst.* 7 (1954) 465.
42. A. H. HEUER and G. L. NORD Jr, "Electron Microscopy in Mineralogy", edited by H. -R. Wenk (Springer-Verlag, Berlin, Heidelberg, New York, 1976) p. 274.
43. H. KROLL and W. F. MÜLLER, *Fortschr. Mineral.* **55** Beiheft 1 (1977) 77.

Received 9 August and accepted 3 November 1978.